





## ORIGINAL ARTICLE

# FOXP4 inhibits squamous differentiation of atypical cells in cervical intraepithelial neoplasia via an ELF3-dependent pathway

Takeo Matsumoto<sup>1</sup> | Takashi Iizuka<sup>1</sup>  | Mitsuhiro Nakamura<sup>1</sup> | Takuma Suzuki<sup>1</sup> | Megumi Yamamoto<sup>1</sup> | Masanori Ono<sup>1,2</sup> | Kyosuke Kagami<sup>1</sup> | Haruki Kasama<sup>1</sup> | Kousho Wakae<sup>3</sup> | Masamichi Muramatsu<sup>3</sup> | Shin-ichi Horike<sup>4</sup> | Satoru Kyo<sup>5</sup>  | Yasuhiko Yamamoto<sup>6</sup> | Yasunari Mizumoto<sup>1</sup>  | Takiko Daikoku<sup>7</sup> | Hiroshi Fujiwara<sup>1</sup> 

<sup>1</sup>Department of Obstetrics and Gynecology, Graduate School of Medical Sciences, Kanazawa University, Kanazawa, Japan

<sup>2</sup>Department of Obstetrics and Gynecology, Tokyo Medical University, Tokyo, Japan

<sup>3</sup>Department of Virology II, National Institute of Infectious Diseases, Tokyo, Japan

<sup>4</sup>Division of Integrated Omics Research, Research Center for Experimental Modeling of Human Disease, Kanazawa University, Kanazawa, Japan

<sup>5</sup>Department of Obstetrics and Gynecology, Shimane University Faculty of Medicine, Izumo, Japan

<sup>6</sup>Department of Biochemistry and Molecular Vascular Biology, Kanazawa University Graduate School of Medical Sciences, Kanazawa, Japan

<sup>7</sup>Division of Animal Disease Model, Research Center for Experimental Modeling of Human Disease, Kanazawa University, Kanazawa, Japan

## Correspondence

Hiroshi Fujiwara and Mitsuhiro Nakamura, Department of Obstetrics and Gynecology, Graduate School of Medical Sciences, Kanazawa University, 13-1 Takaramachi, Kanazawa, Ishikawa 920-8641, Japan.

Emails: [fuji@med.kanazawa-u.ac.jp](mailto:fuji@med.kanazawa-u.ac.jp) (H.F.); [mitsu222@med.kanazawa-u.ac.jp](mailto:mitsu222@med.kanazawa-u.ac.jp) (M.N.)

Takiko Daikoku, Division of Animal Disease Model, Research Center for Experimental Modeling of Human Disease, Kanazawa University, 13-1 Takaramachi, Kanazawa, Ishikawa 920-8640, Japan.

Email: [tdaikoku@kiea.m.kanazawa-u.ac.jp](mailto:tdaikoku@kiea.m.kanazawa-u.ac.jp)

## Funding information

Grants-in-Aid for Scientific Research, Grant/Award Number: 17H04337, 19H01617, 19K22681, 20H03822 and 21H04837; the Japan Agency for Medical Research and Development, Grant/Award Number: 20ck0106549h0001

## Abstract

Although the human papillomavirus (HPV) vaccine is effective for preventing cervical cancers, this vaccine does not eliminate pre-existing infections, and alternative strategies have been warranted. Here, we report that FOXP4 is a new target molecule for differentiation therapy of cervical intraepithelial neoplasia (CIN). An immunohistochemical study showed that FOXP4 was expressed in columnar epithelial, reserve, and immature squamous cells, but not in mature squamous cells of the normal uterine cervix. In contrast with normal mature squamous cells, FOXP4 was expressed in atypical squamous cells in CIN and squamous cell carcinoma lesions. The FOXP4-positive areas significantly increased according to the CIN stages from CIN1 to CIN3. In monolayer cultures, downregulation of FOXP4 attenuated proliferation and induced squamous differentiation in CIN1-derived HPV 16-positive W12 cells via an ELF3-dependent pathway. In organotypic raft cultures, FOXP4-downregulated W12 cells showed mature squamous phenotypes of CIN lesions. In human keratinocyte-derived

**Abbreviations:** CIN, cervical intraepithelial neoplasia; FOXP4, forkhead box transcription factor P4; FOXP4-AS1, FOXP4-antisense RNA 1; HPRT1, hypoxanthine phosphoribosyltransferase 1; HPV, human papillomavirus; HRP, horseradish peroxidase; lncRNA, long noncoding RNA; qPCR, quantitative real-time PCR; ROIs, regions of interest; SCC, squamous cell carcinoma; WAD, weighted average difference.

Takeo Matsumoto and Takashi Iizuka contributed equally to this work.

This is an open access article under the terms of the [Creative Commons Attribution-NonCommercial-NoDerivs](https://creativecommons.org/licenses/by-nc-nd/4.0/) License, which permits use and distribution in any medium, provided the original work is properly cited, the use is non-commercial and no modifications or adaptations are made.

© 2022 The Authors. *Cancer Science* published by John Wiley & Sons Australia, Ltd on behalf of Japanese Cancer Association.

HaCaT cells, FOXP4 downregulation also induced squamous differentiation via an ELF3-dependent pathway. These findings suggest that downregulation of FOXP4 inhibits cell proliferation and promotes the differentiation of atypical cells in CIN lesions. Based on these results, we propose that FOXP4 is a novel target molecule for nonsurgical CIN treatment that inhibits CIN progression by inducing squamous differentiation.

#### KEYWORDS

cervical intraepithelial neoplasia, FOXP4, reserve cells, squamous cell carcinoma, squamous differentiation

## 1 | INTRODUCTION

Uterine cervical carcinoma is one of the most common cancers in young women. It is well-known that HPV plays a central role in the pathogenesis of cervical neoplasia, and that HPV-induced CIN is a key pre-cancerous lesion for uterine cervical SCC.<sup>1</sup> It is well accepted that HPV infection impairs the differentiation of squamous cells, leading to the formation of atypical squamous cell layers.<sup>2,3</sup> This is an initial pathological sign for the morphological diagnosis of CIN.<sup>4</sup> As molecular mechanisms to impair differentiation, HPV16 oncoproteins, E6 and E7, were reported to play an essential role.<sup>5,6</sup> It was proposed that MAML1, NOTCH, and PTPN14 are key molecules that mediate the inhibitory effects of high-risk HPV oncoproteins on squamous differentiation.<sup>3,7,8</sup> However, it is still unknown how differentiation failure is induced from the very early stages in HPV-infected CIN lesions.

During an exploratory study of the pathogenesis of CIN,<sup>9,10</sup> we found that FOXP4 is specifically expressed on atypical squamous cells during CIN progression. Recent studies have suggested that FOXP4 plays important roles in oncogenesis in several tissues, such as non-small-cell lung cancer,<sup>11</sup> prostate cancer,<sup>12,13</sup> and hepatocellular carcinoma.<sup>14</sup> Although FOXP4 has not been reported as a differentiation-related molecule induced by HPV oncoproteins, the FOXP family (FOXP1-4) is also well-known to regulate tissue development or cell differentiation throughout life, playing key roles in embryonic development, cell-cycle regulation, and oncogenesis.<sup>15,16</sup> Among them, FOXP4 has been reported to regulate lung secretory epithelial cell differentiation and regeneration.<sup>17</sup> Consequently, we examined normal uterine cervical tissues and found that FOXP4 is transiently expressed on reserve cells and immature stratified squamous cells during squamous metaplasia. These findings suggest that FOXP4 is a novel key molecule that regulates metaplastic and oncogenic processes of uterine cervical squamous cells.

Based on this background, we further examined the effects of the downregulation of FOXP4 gene expression on the differentiation of CIN1-derived W12 cells, which showed Ca<sup>2+</sup>-dependent squamous differentiation,<sup>18</sup> and clarified regulatory factors of FOXP4 expression, investigating the possibility of FOXP4 being a novel molecular target for nonsurgical CIN therapy. We also confirmed the role of FOXP4 in squamous differentiation using a human

keratinocyte-derived cell line, HaCaT,<sup>19</sup> that was reported to show Ca<sup>2+</sup>-dependent squamous differentiation.<sup>20,21</sup>

## 2 | MATERIALS AND METHODS

### 2.1 | Cell lines

The human cervical dysplasia cell line W12 (RRID:CVCL\_T290, clone 20863),<sup>22</sup> which was authenticated using short tandem repeat (STR) profiling, was gifted by Drs Paul Lambert, Tomomi Nakahara, and Iwao Kukimoto and used in this study. This cell line contains HPV16 episomes. W12 cells were cultured at 37°C under 5% CO<sub>2</sub> in F medium composed of three parts F-12 medium (Sigma-Aldrich) and one part DMEM (Sigma-Aldrich) supplemented with 5% FBS (Sigma-Aldrich), 0.4 µg/ml hydrocortisone, 5 µg/ml insulin, 8.4 ng/ml cholera toxin, 24 µg/ml adenine, 10 ng/ml epidermal growth factor (EGF), 100g/ml streptomycin, and 100IU/ml penicillin.

The immortalized human keratinocytes cell line HaCaT (RRID:CVCL\_0038) was purchased from Cosmo Bio. HaCaT cells were cultured at 37°C under 5% CO<sub>2</sub> in DMEM (Sigma-Aldrich) or calcium-free DMEM (Sigma-Aldrich) supplemented with 10% FBS (Sigma-Aldrich), 100g/ml streptomycin, and 100IU/ml penicillin.

The human cervical squamous carcinoma cell line C33A (RRID:CVCL\_1094), which was authenticated by STR profiling, was used in this study. C33A cells (HPV negative) were cultured at 37°C under 5% CO<sub>2</sub> in DMEM (Sigma-Aldrich) supplemented with 10% FBS (Sigma-Aldrich), 100g/ml streptomycin, and 100IU/ml penicillin.

### 2.2 | Samples

Tissue samples from the uterine cervix were obtained from 57 patients who had undergone hysterectomy or conization at Kanazawa University Hospital. They included five cases of normal cervical tissues, eight cases of CIN1, 12 cases of CIN2, 19 cases of CIN3, and 13 cases of SCC. All surgical specimens were fixed in 20% formalin and embedded in paraffin. The tissue sections (4 µm) were stained using routine histopathological techniques for diagnosis and were reviewed by two pathologists. Sequential tissue sections of the same lesions were used for the immunohistochemical study.

## 2.3 | Immunohistochemical staining

Tissue localizations of FOXP4, ELF3, cytokeratin 10 (KRT10), and Involucrin (IVL) were immunohistochemically determined using the avidin–biotin–peroxidase complex method according to the manufacturer's instructions (VECTASTAIN ABC Kit, Vector Laboratories). The slides were incubated overnight at 4°C with either one of the primary antibodies, anti-FOXP4 rabbit polyclonal antibody (1:200, HPA007176, [RRID:AB\\_1078911](#), Sigma-Aldrich), anti-ELF3 rabbit polyclonal antibody (1:200, [RRID:AB\\_1078756](#), HPA003479, Sigma-Aldrich), or for 1 h at room temperature with either one of primary antibodies, anti-KRT10 rabbit monoclonal antibody (1:20,000, clone EP1607IHCY, Ab76318, [RRID:AB\\_1523465](#), Ab76318, Abcam), and anti-IVL rabbit polyclonal antibody (1:100, Ab53112, [RRID:AB\\_880813](#), Abcam). Control staining was performed by replacing the primary antibody with normal rabbit or mouse serum solution.

## 2.4 | Assessment of FOXP4 expression profiles in CIN lesions

All CIN and cancer lesions were examined in a magnified area ( $\times 100$ ) for quantification. Images were captured using an Olympus BX50 microscope and a DP72 Olympus digital camera, and cellSens standard 1.5 software (Olympus). We selected the area showing the most severe lesions in each case, and the corresponding epithelial lesions were delineated as ROIs. Both areas of FOXP4-positive cells and hematoxylin-stained cells in each ROI were calculated, the ratio of the FOXP4-positive and hematoxylin-stained areas was defined as the FOXP4-positive rate, and values were normalized using National Institutes of Health (NIH) ImageJ software, as described previously.<sup>9</sup>

## 2.5 | Western blot analysis

To analyze the protein expression level of FOXP4 in clinical samples, protein lysates were extracted with RIPA buffer (Cell Signaling Technology Inc.). Each lysate was electrophoresed on 7.5% SDS-PAGE gels and then transferred to nitrocellulose membranes. The transferred membranes were incubated with primary antibody against FOXP4 (1:1000, [RRID:AB\\_2262825](#), 16772-1-AP, Proteintech Group Inc.) or  $\beta$ -Actin (1:5000, [RRID:AB\\_630835](#), C-11, Santa Cruz Biotechnology) overnight at 4°C. Secondary horseradish peroxidase (HRP)-conjugated antibody was applied for 1 h at room temperature. The blots were visualized using an enhanced chemiluminescence system and ECLTM Western Blotting Detection Reagents (GE Healthcare).

## 2.6 | RT-PCR and quantitative real-time PCR analysis

Total RNA was extracted from clinical samples and the cell line using the RNeasy Mini kit (Qiagen) according to the manufacturer's instructions. The RNA was reverse transcribed to cDNA using the PrimeScript™ RT-PCR kit (Takara Bio Inc.). HPRT1 was used for the control. The cDNA was amplified using specific primers, forward and reverse primers, which are listed in [Table 1](#). The conditions for PCR cycling were 95°C for 30s and 36 cycles of 5 s at 95°C, followed by an annealing and extension step at 60°C for 20s. Quantitative real-time PCR (qPCR) analysis was performed using the Mx3000P real-time PCR system (Agilent Stratagene), according to the manufacturer's instructions. The mean  $\pm$  SD of three independent experiments is shown.

TABLE 1 Primer sequences for RT-PCR and quantitative real-time PCR

| Gene   | Forward primers          | Reverse primers           |
|--------|--------------------------|---------------------------|
| FOXP4  | GTTACCAGGATGTTGCGCT      | CTCCGCTTCTGATACTCCCG      |
| KRT1   | ATTTCTGAGCTGAATCGTGTGATC | CTTGGCATCCTTGAGGGCATT     |
| KRT10  | TGATGTGAATGTGGAAATGAATGC | GTAGTCAGTTCCTTGCTCTTTTCA  |
| IVL    | GGGTGGTTATTTATGTTTGGGTGG | GCCAGGTCCAAGACATTCAAC     |
| HES1   | AGCTGGAGAAGGCGGACATT     | CATTGATCTGGGTGATGCAG      |
| HES2   | AGAACTCCAAGTCTCGAAGC     | CGGTCATTTCCAGGACGCTCT     |
| HES5   | CCGGTGGTGGAGAAGATG       | TAGTCTGGTGCAGGCTCTT       |
| HEY1   | GAGAAGCGCCGACGAGACCG     | GGCGTGCGGTCAAAGTAACCTTT   |
| ELF3   | CAACTATGGGGCCAAAAGAA     | TTCCGACTCTGGAGAACCTC      |
| TGM1   | TCAGACGCTGGGGAGTTC       | GGTCCGCTACCAATCTG         |
| GRHL3  | GCCAGTTCTACCCCGTCA       | GTCAATGACCCGCTGCTT        |
| SPRR1  | CCAGCAGAAGACCAAGCAGAA    | GCAAATGGGACTCATACGCAGAATG |
| NOTCH1 | CAATGTGGATGCCGAGTTGTG    | CAGCACCTTGCGGTCTCGTA      |
| NOTCH2 | AAAAATGGGGCCAACCGAGAC    | TTCATCCAGAAGGCGCACAA      |
| NOTCH3 | AGATTCTCATCCGAAACCGCTCTA | GGGGTCTCCTCTTGCTATCCTG    |
| NOTCH4 | CAGCCCAAGCAGATATGTAAGGA  | CGTCCAACCCACGTCACA        |
| HPRT1  | GCCCTGGCGTCGTGATTAGT     | CGAGCAAGACGTTTCAGTCTCTGTC |

## 2.7 | DNA microarray analysis

One-color microarray-based gene expression array analysis was performed according to the manufacturer's instructions. Briefly, labeled cDNA was prepared from 0.2 µg RNA using the Low Input Quick Amp Labeling Kit (Agilent Technologies). Samples were hybridized to SurePrint G3 Human GE microarray 8x60K Ver. 3.0 (G4845A#72363, Agilent Technologies), and scanned on an Agilent DNA Microarray Scanner (G2539A) using the one-color scan setting for 1x60k array slides (Agilent Technologies). The scanned images were analyzed using Feature Extraction Software 11.0.1.1 (Agilent Technologies). Data were normalized and filtered with three filters using GeneSpring software v.12.1 (Agilent Technologies).

Differentially expressed genes were extracted from normalized microarray intensity data using the weighted average difference (WAD) ranking method.<sup>23</sup> This method is a statistical approach based on the fold-change method that uses not only the difference in gene expression, but also the signal intensity in microarrays. Fold change was calculated by dividing the NC-shRNA value by the FOXP4-shRNA value.

## 2.8 | Lentiviral transfection

RNA interference to reduce FOXP4 gene expression was performed using lentivirus particles of MISSION® small hairpin RNA (FOXP4-shRNA1-5: TRCN0000285257, TRCN0000274833, TRCN0000274834, TRCN0000274832, and TRCN0000274894, respectively), purchased from Sigma-Aldrich. Nontarget control lentivirus particles of MISSION® shRNA (NC-shRNA: SHC202V) were also purchased from Sigma-Aldrich. The W12 cells transfected with FOXP4-shRNA (MOI = 20) or NC-shRNA (MOI = 20) were selected by subsequent incubation for 2 weeks using puromycin.

## 2.9 | siRNA transfection

The W12 cells transfected with FOXP4-shRNA were transfected with Silencer® Select siRNAs following the manufacturer's protocol using Lipofectamine RNAiMAX (13778075, Thermo Fisher Scientific Inc.). siRNAs for *ELF3* (s4623 and s4624, Thermo Fisher Scientific), *NOTCH3* (s9640 and s9641, Thermo Fisher Scientific), and the corresponding Silencer® Select Negative Control No. 1 (AM4635, Thermo Fisher Scientific) were used.

## 2.10 | Cell proliferation assay

The treated W12 cells were seeded into 96-well plates at  $5 \times 10^3$  cells per well. After a 24 to 96-h incubation, cell proliferation was determined using Cell Proliferation Reagent WST-1 (Roche) according to the manufacturer's instructions. All experiments were performed in triplicate.

## 2.11 | Analysis of stratified structures in W12 cells under monolayer cultures

The W12 cells transfected with FOXP4-shRNA and NC-shRNA were cultured on glass chamber slides (Lab-Tek® II, Thermo Fisher Scientific). A slide with 80% confluent cells was fixed in 4% paraformaldehyde and stained by Hoechst® 33342 (Thermo Fisher Scientific). The stained nuclei were scanned using a confocal laser scanning microscope (LSM510; Carl Zeiss) and sagittal images were reconstructed. Horizontal images (x100) were captured using an Olympus BX50 microscope and a DP72 Olympus digital camera, and cellSens standard 1.5 software (Olympus). The sites showing overlapping nuclei were defined as cell-overlapping zones, and the total area of overlapping zones was calculated using NIH ImageJ software.

## 2.12 | Organotypic raft cultures

Organotypic rafts were cultured as previously described.<sup>24,25</sup> Briefly,  $2.0 \times 10^6$  3T3J2 fibroblasts were suspended in a collagen gel composed of 80% collagen, 10% 10x DMEM, and 10% equilibration buffer, and the mixture was allowed to solidify. Then,  $2.0 \times 10^6$  W12 cells transfected with FOXP4-shRNA or NC-shRNA in F medium with 1 µg/ml puromycin were seeded onto the surface of the gel. The next day, the gel was lifted onto a metal grid in a culture dish and exposed to the F medium without EGF from below and air from above. The rafts were incubated at 37°C and the medium was changed every other day. After 14 days, rafts were harvested, fixed in 4% paraformaldehyde and embedded in paraffin, sectioned, stained with hematoxylin and eosin, and used for immunohistochemical staining.

## 2.13 | Effects of high concentration of calcium and FOXP4 on squamous differentiation in HaCaT cells

To induce differentiation, wild-type HaCaT cells were seeded into 12-well plates at  $1.0 \times 10^5$  cells per well and incubated for 24 h in calcium-free culture medium, and then further cultured in the culture medium (1.8 mM  $\text{CaCl}_2$ ) for up to 72 h. The transfected HaCaT cells were seeded in 12-well plates at  $1.0 \times 10^5$  cells per well and cultured in calcium-free culture medium to eliminate the effects of calcium on promoting differentiation.

## 2.14 | Statistical analysis

The differences in the expression of squamous differentiation- and NOTCH signal-related genes between the treated and control W12 and HaCaT cells were analyzed using paired t-test or ANOVA followed by Dunnett test using statistical software (SPSS Statistics version 25.0, IBM). The dose-dependent assay and cell proliferation assay were also analyzed using ANOVA followed using Dunnett test. A p-value of <0.05 was considered significant.

### 3 | RESULTS

#### 3.1 | FOXP4 is expressed in columnar epithelial, reserve, and immature squamous cells in the normal uterine cervix

In normal cervical tissues, FOXP4 expression was undetectable in the mature stratified squamous cell layers (Figure 1A-a). Intranuclear localization of FOXP4 was observed in the endocervical glandular epithelial cells (Figure 1A-b, arrows). At the squamocolumnar junction (Figure 1A-c), FOXP4 expression was undetectable in the mature stratified squamous cell layers

(arrowheads), whereas it was clearly expressed in columnar epithelial cells (arrows). In the region undergoing metaplasia, a single layer of reserve cells (Figure 1A-d, e, arrows) lined just beneath the columnar epithelial cell layer. Immature stratified squamous cells (arrowheads in Figure 1A-f) were constructed over reserve cells (arrows in Figure 1A-f).<sup>26</sup> Intranuclear localization of FOXP4 was clearly detected in the reserve cells and immature stratified squamous cells. Considering that FOXP4 expression disappeared in the mature stratified squamous cells at the established squamocolumnar junction (Figure 1A-a), its transient expression on immature stratified squamous cells suggests that FOXP4 is related to the squamous metaplasia from columnar epithelial cells.

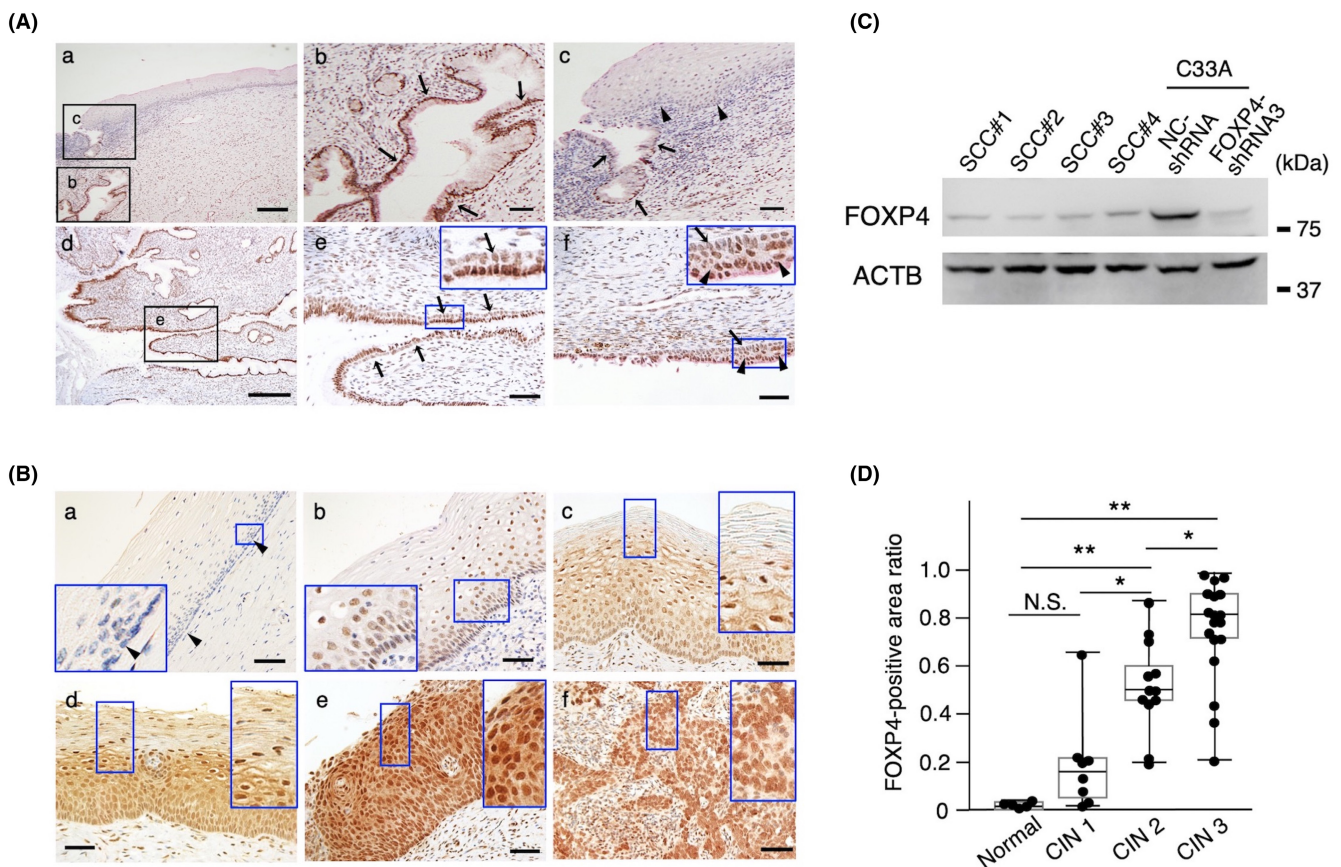


**FIGURE 1** The expression profiles of FOXP4 on normal tissues and CIN and SCC lesions by immunohistochemistry. (A) Stained using anti-FOXP4 Ab (HPA007176). (A-a) Around a mature squamocolumnar junction (black box c); (A-b, A-c) Magnified images of the black square (b) and (c) of (a); (A-d) Endocervical glands undergoing squamous metaplasia. (A-e) Magnified image of the black d square. (A-f) An immature stratified squamous cell layer. (A-b) Intranuclear expression of FOXP4 was observed in endocervical glandular epithelial cells. (A-c) FOXP4 expression was undetectable in the mature stratified squamous cell layers (arrowheads), whereas it was clearly expressed in columnar epithelial cells (arrows). (A-e) FOXP4 was detected in the reserve cells (arrows). (A-f) Immature stratified squamous cells (arrowheads) are newly constructed from reserve cells (arrows) and expressed FOXP4 (arrowheads). Scale bars, 200  $\mu$ m (d), 100  $\mu$ m (a), and 50  $\mu$ m (b, c, e, f). (B) FOXP4 expression in normal stratified squamous layer (B-a), CIN1 (B-b), CIN2 (B-c, B-d), CIN3 (B-e), and SCC (B-f). FOXP4 was undetectable in the mature stratified squamous cell layers (B-a, arrowheads), weakly detected in CIN1 (B-b), and moderately in CIN2 (B-c). The positive area was extended beyond the atypical cell layer in some CIN2 cases (B-d). High FOXP4 expression was observed in CIN3 (B-e) and SCC (B-f). Scale bars, 50  $\mu$ m (a-f). (C) Western blot analysis of FOXP4 in SCC tissues. The protein bands corresponding to the estimated molecular mass of FOXP4 protein, 80 kDa, were detected. Mock-treated and FOXP4-shRNA3-treated C33A cells were used for positive and negative controls.  $\beta$ -Actin (ACTB) was used as a control. (D) The positive ratios of FOXP4 expression significantly increased according to CIN stages. The data were analyzed using Kruskal-Wallis test followed by Steel-Dwass test and shown as the median and interquartile range. \*  $p < 0.05$ ; \*\*  $p < 0.01$ ; N.S., not significant

**FIGURE 2** Downregulation of FOXP4 inhibits proliferation in W12 cells. (A) Intranuclear localization of FOXP4 was observed in W12 cells. Treatment with FOXP4-hRNA1 and four significantly reduced the mRNA (B) and protein (C) expression of FOXP4. (D) WST-1 assay showed that proliferation was significantly decreased in W12 cells treated with FOXP4-shRNA. The data were analyzed using ANOVA followed using Dunnett test. \* $p < 0.05$ ; \*\* $p < 0.01$ ; N.S., not significant. Scale bars, 50  $\mu\text{m}$ . Three separate experiments were performed and bars represent SD (B). The results are shown as means of individual experiments ( $N = 3$ ) and bars represent SEM (D)

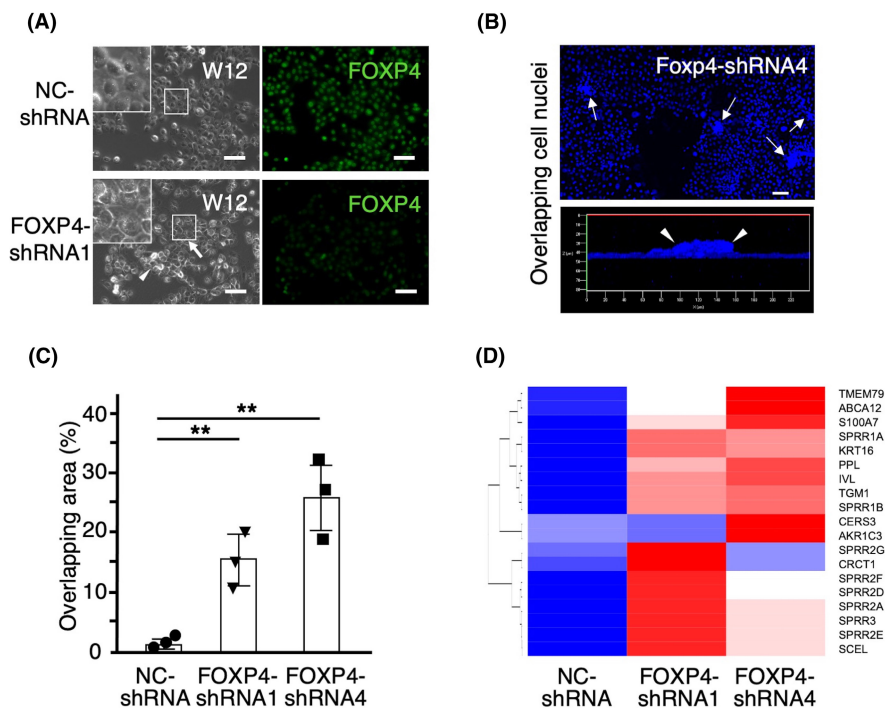
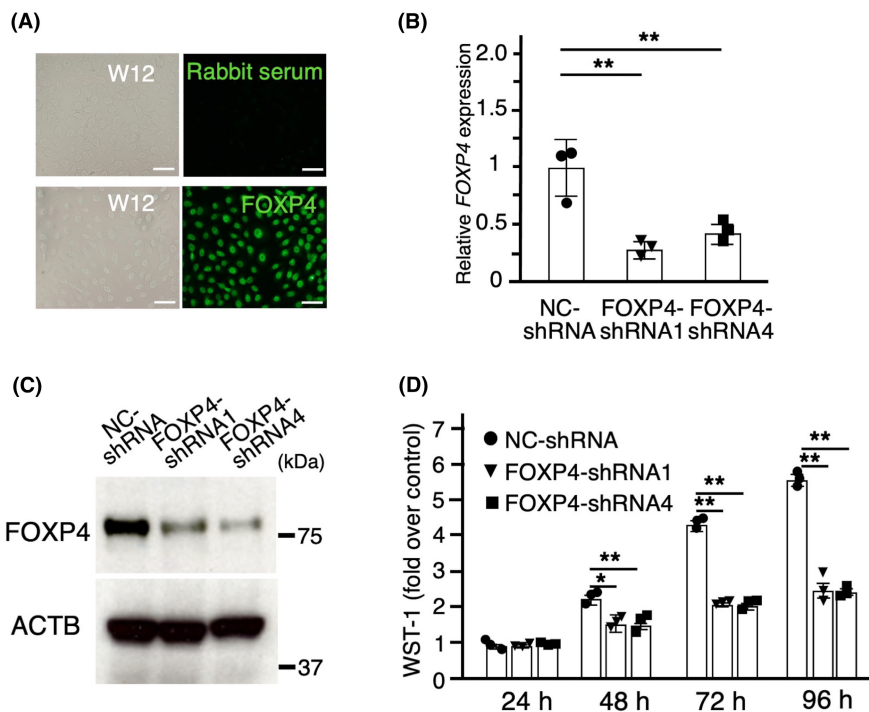


**FIGURE 3** Morphological and gene expression changes by downregulation of FOXP4 in W12 cells. (A) Control W12 cells were oval shaped, whereas FOXP4-shRNAs-treated cells show the growth of islands that contain flattened cells (arrows) and stratified structures (arrowheads) with reduction of FOXP4 expression. (B) Stratified structures (arrowheads) were analyzed using sagittal images. (C) The calculated areas of overlapping nuclei (arrows in B) are significantly larger in FOXP4-shRNAs-treated cells. (D) Heatmap of the microarray shows enhanced epithelial differentiation-related genes in FOXP4-shRNA-treated cells. The results are shown as means of individual experiments ( $N = 3$ ) and bars represent SEM. The data were analyzed using ANOVA followed by Dunnett test. \* $p < 0.05$ ; \*\* $p < 0.01$ ; N.S., not significant. Scale bars, 50  $\mu\text{m}$  (A); and 100  $\mu\text{m}$  (B)

### 3.2 | FOXP4 is expressed in atypical cells in CIN and SCC lesions

In mature stratified squamous cell layers of the normal uterine cervix, FOXP4 expression was undetectable (Figure 1B-a, arrowheads). In the CIN1 lesions, FOXP4 was weakly detected (Figure 1B-b). In the CIN2 lesions, FOXP4 was moderately expressed in atypical cells (Figure 1B-c), and its positive area was extended beyond the atypical cell layer in some cases (Figure 1B-d). In the CIN3 lesions, FOXP4 was intensely expressed in the atypical cells throughout the whole layer (Figure 1B-e). High FOXP4 expression was also observed in all cases of SCC (Figure 1B-f). Western blotting detected the protein bands corresponding to the estimated molecular mass of FOXP4, 80kDa, in the four tissue samples derived from SCC (Figure 1C). Mock-treated and FOXP4-shRNA3-treated C33A cells, a cell line derived from cervical squamous cells,<sup>27</sup> were used for positive and negative controls. FOXP4-positive image analysis confirmed that FOXP4 expression was significantly increased according to the CIN stages from CIN1 to CIN3 (Figure 1D).

### 3.3 | Downregulation of FOXP4 inhibits proliferation and promotes squamous differentiation of W12 cells

To further investigate the role of FOXP4 in dysplastic cervical cells, we adopted a cell line, W12, established from an HPV16-positive CIN1 region.<sup>22</sup> Intracellular localization of FOXP4 was verified in W12 cells (Figure 2A). The mRNA expression of FOXP4 was attenuated by treatment with shRNA for FOXP4 (FOXP4-shRNA1 and 4) (Figure 2B). This treatment reduced the FOXP4 protein expression (Figure 2C) and decreased cell proliferation (Figure 2D).

FOXP4 reduction also induced mature squamous phenotypes in W12 cells, showing a flattened appearance in places (arrows in Figure 3A). Stratified growth with island formation, which is a typical sign of differentiation toward stratified squamous cells, was also induced (arrowheads in Figure 3A). Sagittal images of the stained nuclei reconstructed using a confocal laser scanning microscope clearly showed the stratified structures (Figure 3B). The cell-overlapping zones calculated from captured horizontal images of the stained nuclei were significantly increased in FOXP4-shRNA-treated W12 cells (Figure 3C).

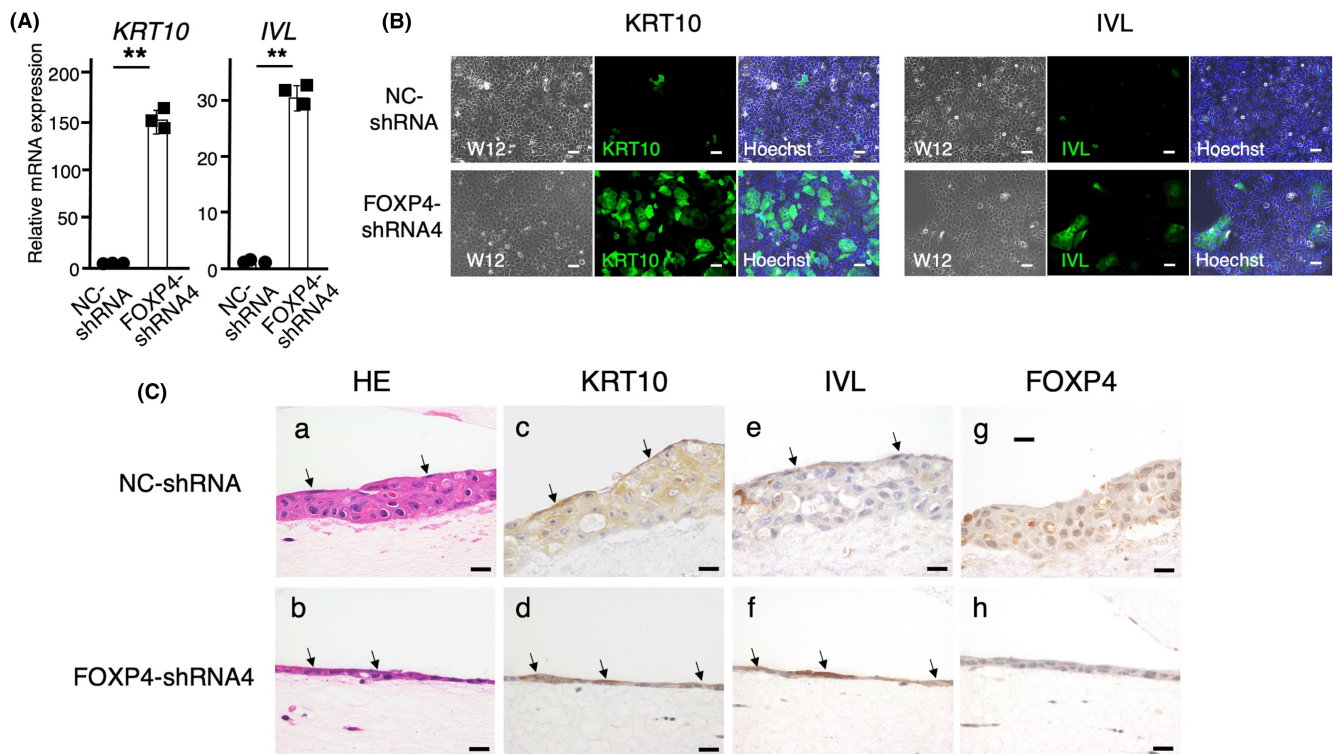


**FIGURE 4** Downregulation of FOXP4 promotes squamous differentiation in W12 cells. FOXP4-shRNA4 treatment increased mRNA (A) and protein (B) expression of KRT10 and/or IVL. (C) A raft culture of W12 cells. (C-a) Control cells reproduced the whole layers of CIN lesions and squamous-like cells (arrows) in the uppermost layer. (C-b) FOXP4-shRNA4-treated cells developed into a few layers of flattened cells (arrows), which mimic the superficial layer of CIN lesions. KRT10 (C-c) and IVL (C-e) expression were low or moderate in the squamous-like cells (arrows) in control cells. High expression of KRT10 (C-d) and IVL (C-f) is detected in the stratified flattened cells (arrows) in FOXP4-shRNA4-treated cells. FOXP4 expression was suppressed in W12 cells treated with FOXP4-shRNA (C-g and C-h). Three separate experiments were performed and bars represent SD. The data were analyzed using paired *t*-test. \**p* < 0.05; \*\**p* < 0.01; N.S., not significant. Scale bars, 50 μm

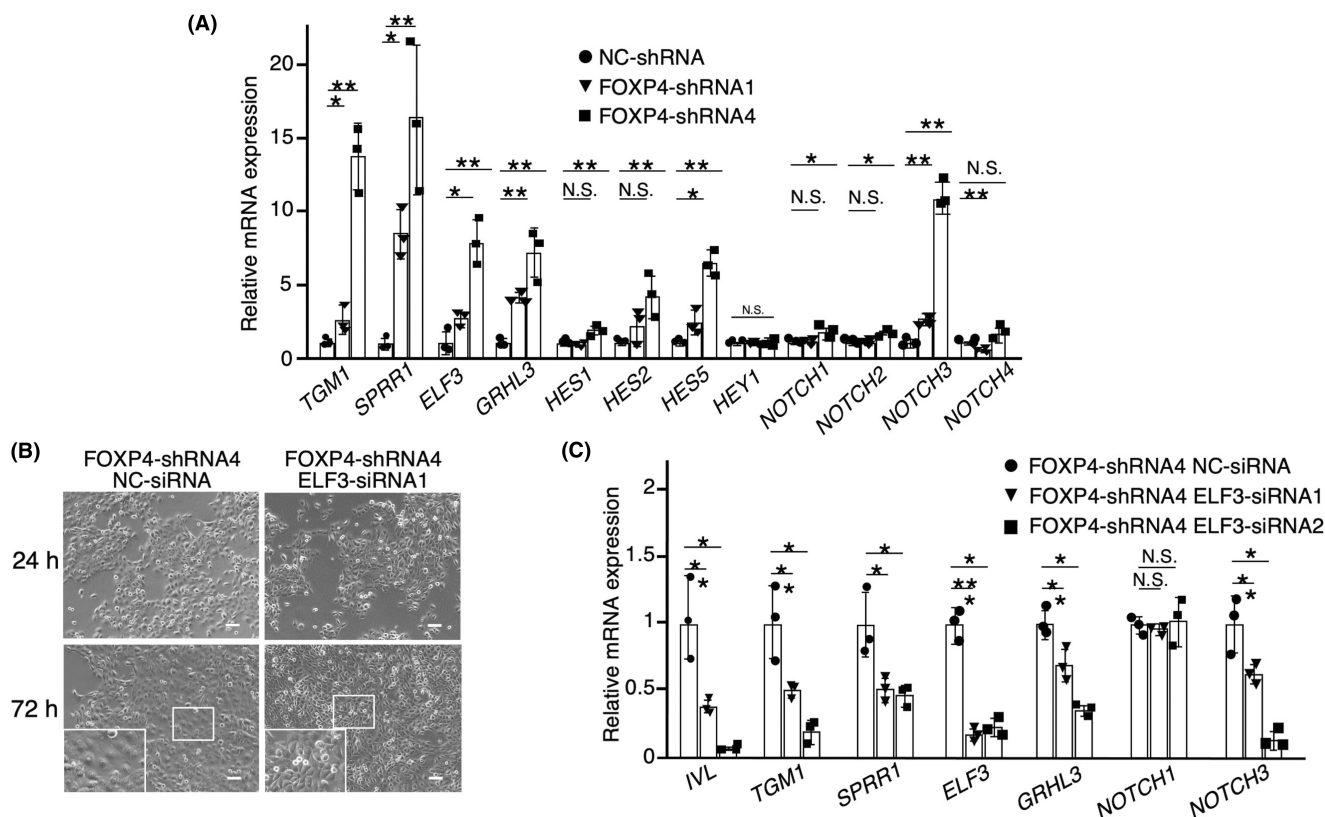


**FIGURE 5** Downregulation of ELF3 recovered FOXP4-induced inhibition of squamous differentiation in W12 cells. (A) FOXP4-shRNA4 treatment altered gene expression of squamous differentiation-related genes. The mRNA expression of *TGM1*, *SPRR1*, *ELF3*, *GRHL3*, *HES2*, *HES5*, *NOTCH3*, and slightly *NOTCH1* and *NOTCH2*, but not *NOTCH4*, was significantly promoted. Knockdown of *ELF3* by siRNAs inhibited morphological changes in squamous differentiation in FOXP4-shRNA-treated W12 cells (B) and the expression of *TGM1*, *SPRR1*, *IVL*, and *GRHL3* as well as *NOTCH3*, but not *NOTCH1* (C). Three separate experiments were performed and bars represent SD. The data were analyzed using ANOVA followed using Dunnett test. \* $p < 0.05$ ; \*\* $p < 0.01$ ; N.S., not significant. Scale bars, 100 μm

To identify the FOXP4-regulated molecules in W12 cells, microarray analysis was performed using the WAD ranking method.<sup>23</sup> The top three groups by gene ontology analysis were: (1) epidermis development, (2) epidermal cell differentiation, and (3) keratinocyte differentiation. Heatmaps of epithelial differentiation-related genes are shown in Figure 3D.

Using RT-qPCR analysis, mRNA expression of differentiation markers of keratinocytes, *KRT10* and *IVL* were significantly increased in FOXP4-shRNA-treated W12 cells (Figure 4A). The increase in protein expression was confirmed using immunofluorescence staining (Figure 4B).

We further performed a raft culture in which transformed cell lines exhibit dysplastic morphologies similar to the preneoplastic lesions seen in vivo.<sup>24</sup> W12 cells treated with NC-shRNA developed a stratified three-dimensional structure that consisted of atypical cells without mature differentiation (Figure 4C-a), which morphologically reproduced all layers of CIN lesions. *KRT10* and *IVL* expressions were low in the stratified layer and moderate in the uppermost thin layer (Figure 4C-c and e). Conversely, W12 cells treated with FOXP4-shRNA developed into a few layers of flattened cells, which mimicked the superficial layer of CIN lesions (Figure 4C-b). High expression of *KRT10* and *IVL* was detected in the stratified flattened

cells (Figure 4C-d, f). These findings suggest that W12 cells treated with FOXP4-shRNA are consistent with the further differentiated phenotype in CIN lesions.

### 3.4 | Downregulation of ELF3 and NOTCH3 recovered FOXP4-induced inhibition of squamous differentiation in W12 cells

Then, as NOTCH was proposed as key molecules to inhibit squamous differentiation by high-risk HPV oncoproteins,<sup>3,28</sup> we investigated squamous differentiation-related and NOTCH signal-related gene expression in FOXP4-shRNA-treated W12 cells using RT-qPCR, and found that mRNA expression of *TGM1*, *SPRR1*, *ELF3*, *GRHL3*, *HES2*, *HES5*, and *NOTCH3* were significantly promoted (Figure 5A).

Knockdown of *ELF3* by siRNAs inhibited morphological changes in squamous differentiation in FOXP4-shRNA-treated W12 cells (Figure 5B) and the expression of *TGM1*, *SPRR1*, *IVL*, and *GRHL3* as well as *NOTCH3*, but not *NOTCH1* (Figure 5C). Additional application of siRNAs targeting *NOTCH3* showed the inhibition of morphological changes in squamous differentiation (Figure 6A) and gene induction of *HES2*, *HES5*, and *IVL* expression (Figure 6B). These results



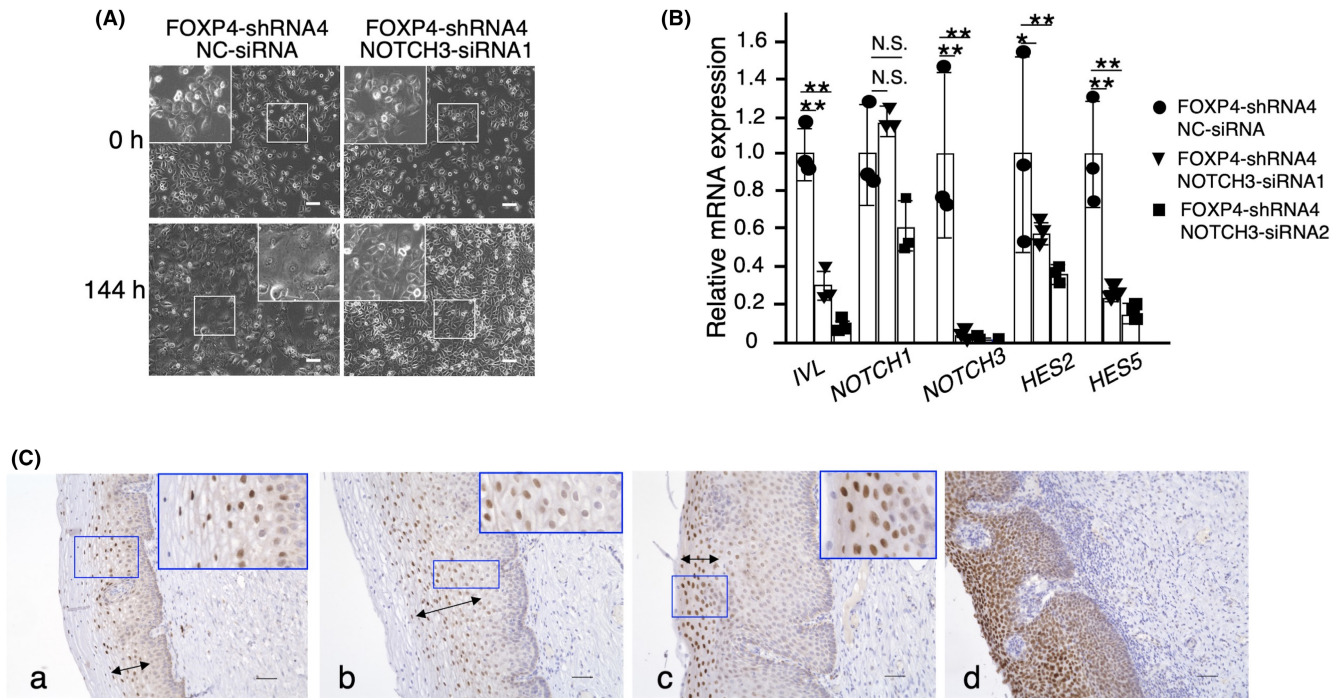


**FIGURE 6** Downregulation of NOTCH3 recovered FOXP4-induced inhibition of squamous differentiation in W12 cells. Additional application of siRNAs targeting *NOTCH3* in FOXP4-shRNA-treated W12 cells shows the inhibition of morphological changes in squamous differentiation (A) and gene induction of *HES2*, *HES5*, and *IVL* expression (B). (C) ELF3 was dominantly expressed in the intermediate layer in normal cervical tissues (C-a), and in the cells that had undergone squamous differentiation in CIN1 (C-b) and CIN2 (C-c) lesions (double-headed arrows), which corresponded to the intermediate layer. In CIN3, ELF3 was constitutively expressed on atypical cells from the parabasal layer (d). Three separate experiments were performed and bars represent SD. The data were analyzed using ANOVA followed by Dunnett test. \* $p < 0.05$ ; \*\* $p < 0.01$ ; N.S., not significant. Scale bars, 100  $\mu\text{m}$  (A) and 50  $\mu\text{m}$  (C)

suggested that FOXP4 suppresses squamous differentiation by downregulating ELF3 and NOTCH3 expression.

In accordance with this speculation, ELF3 was dominantly expressed in the intermediate layer in normal cervical tissues (Figure 6C-a), and in the cells that underwent squamous differentiation in CIN1 (Figure 6C-b) and CIN2 (Figure 6C-c) lesions (double-headed arrows), which corresponded to the intermediate layer. As shown in Figure 1, FOXP4 was mainly expressed on atypical basal to parabasal cells. Consequently, this suggests that the expression of FOXP4 had decreased, whereas that of ELF3 had increased when parabasal-like cells had differentiated into intermediate-like cells. This expression profile is consistent with the results of the W12 cell culture, showing that ELF3 is inversely expressed with FOXP4 during squamous differentiation. In CIN3, ELF3 was constitutively expressed on atypical cells from the parabasal layer (Figure 6C-d).

### 3.5 | Downregulation of FOXP4 promotes squamous differentiation in HaCaT cells

HaCaT is a spontaneously transformed immortal keratinocyte cell line from adult human skin.<sup>19</sup> Extracellular calcium concentration was reported to induce squamous differentiation in HaCaT cells.<sup>21</sup> In the recommended maintaining culture condition (1.8 mM  $\text{CaCl}_2$ ), intranuclear localization of FOXP4 in HaCaT cells was verified by

immunofluorescence staining (Figure 7A, in the middle panel). Under calcium-free culture conditions, the intranuclear expression of FOXP4 in HaCaT cells was increased (Figure 7A, in the lower panel). Accordingly, mRNA expression of FOXP4 was reduced under the maintaining culture condition (1.8 mM  $\text{CaCl}_2$ ) along with an increase in *IVL* expression (Figure 7B).

The mRNA expression of FOXP4 was attenuated following treatment with shRNA for FOXP4 (FOXP4-shRNA3 and -4; Figure 7C). Western blot analysis (Figure 7D) confirmed the reduction in FOXP4 protein expression. RT-qPCR analysis demonstrated that the mRNA expression of *KRT1* and *KRT10* was significantly increased in FOXP4-shRNA-treated HaCaT cells (Figure 7E).

We also observed that the mRNA expression of *SPRR1*, *ELF3*, *GRHL3*, *HES1*, and *HES5* was significantly promoted (Figure 8A). Knockdown of *ELF3* inhibited gene induction of the transcriptional factor and squamous differentiation markers *TGM1*, *SPRR1*, *IVL*, and *GRHL3* as well as *NOTCH3*, but not *NOTCH1* (Figure 8B).

## 4 | DISCUSSION

To our knowledge, this study is the first to demonstrate expression profiles of FOXP4 in the human normal uterine cervix. Around the squamocolumnar junction, FOXP4 protein is expressed in reserve cells and in the immature stratified squamous cells that are derived

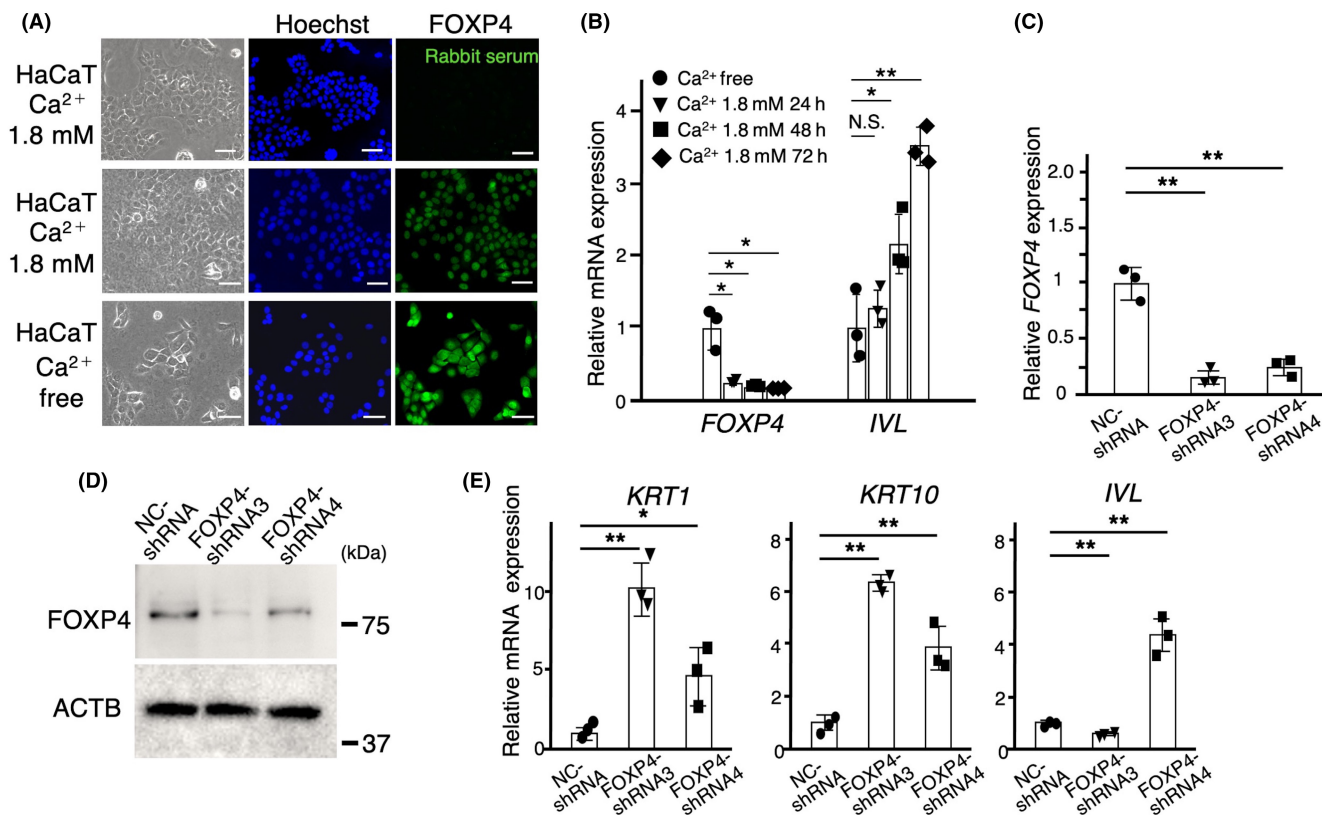


**FIGURE 7** Downregulation of FOXP4 promotes squamous differentiation in HaCaT cells. In the recommended maintaining culture condition (1.8 mM CaCl<sub>2</sub>), intranuclear localization of FOXP4 in HaCaT cells was verified using immunofluorescence staining (A, middle panel). Under calcium-free culture conditions, the intranuclear expression of FOXP4 in HaCaT cells was increased (A, lower panel). (B) mRNA expression of FOXP4 is reduced under the maintaining culture condition (1.8 mM CaCl<sub>2</sub>) along with increase in IVL expression. (C) mRNA expression of FOXP4 is attenuated by treatment with shRNA for FOXP4 (FOXP4-shRNA3 and 4). (D) Western blot analysis confirmed the reduction in FOXP4 protein expression. (E) RT-qPCR analysis demonstrated that the mRNA expression of KRT1 and KRT10 was significantly increased in FOXP4-shRNA-treated HaCaT cells. Three separate experiments were performed and bars represent SD. The data were analyzed using ANOVA followed by Dunnett test. \* $p < 0.05$ ; \*\* $p < 0.01$ ; N.S., not significant. Scale bars, 50 μm

from reserve cells.<sup>26</sup> However, FOXP4 expression disappeared in the mature stratified squamous cells at the established squamocolumnar junction. This transient expression suggests that FOXP4 is related to the squamous cell metaplasia from columnar epithelial cells. For the murine lung, it has been reported that FOXP1 and FOXP4 cooperatively regulate the differentiation pathway of lung secretory epithelial cells toward goblet cells, partially through anterior gradient protein 2 (Agr2),<sup>17</sup> suggesting an important role for FOXP4 in the determination of epithelial cell differentiation. Intriguingly, it was reported that Agr2 was identified as one of the squamocolumnar junction-specific proteins of the human cervix by gene expression screening.<sup>29,30</sup> Although the precise mechanisms remain unknown, this evidence supports the above speculation that FOXP4 is involved in the process of squamous metaplasia from columnar epithelium. Notably, the present study showed that the intensity of FOXP4 expression in atypical cells in CIN lesions significantly increased according to the CIN stages and its high expression was constantly observed in SCC. These expression profiles suggest the involvement of FOXP4 in the process of CIN developing into SCC.

Suppression of FOXP4 gene expression induced morphological changes in W12 cells, which are compatible with squamous

differentiation. In addition, gene expression of squamous differentiation markers, KRT1, KRT10, and IVL, was significantly increased in W12 cells following the knockdown of FOXP4. This treatment also significantly reduced the proliferation of W12 cells. These results indicated that FOXP4 is one of the important factors regulating proliferation and differentiation in W12 cells, and suggested that FOXP4 promotes proliferation and inhibits the differentiation of atypical squamous cells in CIN lesions. From these findings, we consider that the cellular changes induced by FOXP4 suppression correspond to the differentiating process observed in the superficial layer of CIN lesions.

To confirm the above speculation, we used a raft culture that is an organotypic three-dimensional culture system. In this culture, control W12 cells (treated with NC-shRNA) developed into several layers of a stratified structure containing atypical cells without mature differentiation. This was compatible with the whole layers of CIN lesions. In contrast, FOXP4-suppressed W12 cells developed into a few layers of stratified flattened cells, whose morphological characteristics were compatible with the superficial layer of CIN lesions. As the downregulation of FOXP4 attenuated the proliferation of W12 cells, these findings suggested that the inhibition of FOXP4

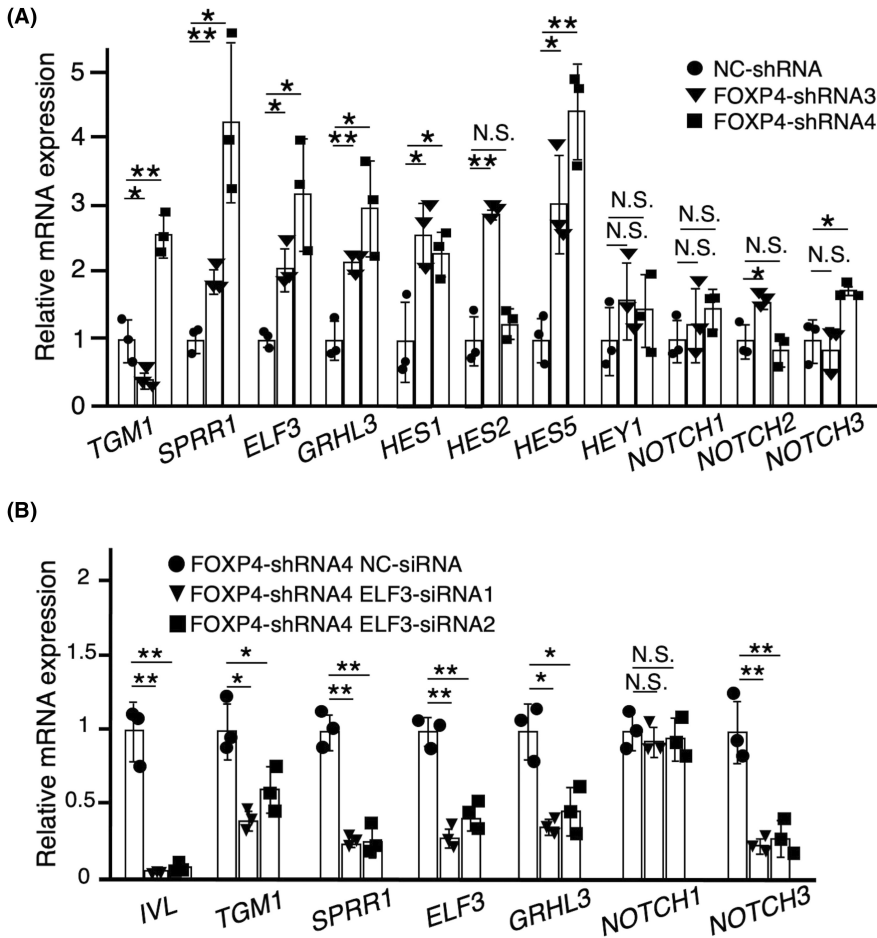


**FIGURE 8** Downregulation of ELF3 recovered FOXP4-induced inhibition of squamous differentiation in HaCaT cells. (A) In FOXP4-shRNA-treated HaCaT cells, mRNA expression of *SPRR1*, *ELF3*, *GRHL3*, *HES1*, and *HES5* was significantly promoted. (B) Knockdown of *ELF3* inhibited gene induction of the transcriptional factor and squamous differentiation markers *TGM1*, *SPRR1*, *IVL*, and *GRHL3* as well as *NOTCH3*, but not *NOTCH1*. Three separate experiments were performed and bars represent SD. The data were analyzed using ANOVA followed by Dunnett test. \* $p < 0.05$ ; \*\* $p < 0.01$ ; N.S., not significant

expression can suppress the growth of atypical stratified layers in CIN lesions by inducing further differentiation toward the mature phenotype of squamous cells.

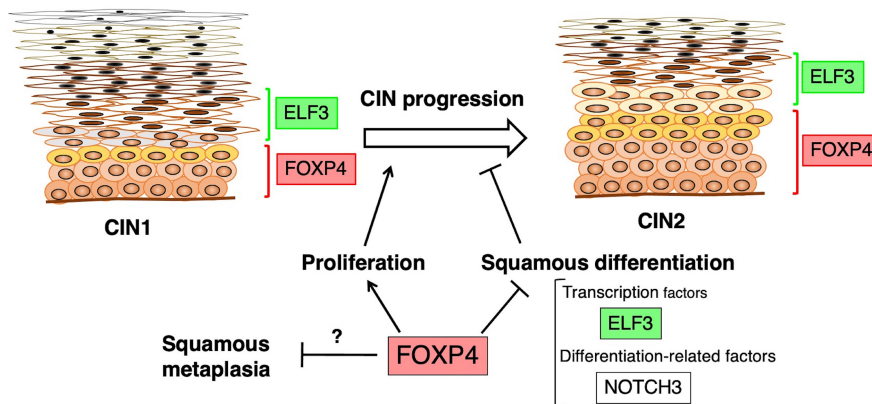
It is well accepted that HPV infection impairs the differentiation of squamous cells, leading to the formation of atypical squamous cell layers.<sup>3</sup> This is an initial pathological sign for the morphological diagnosis of CIN. As molecular mechanisms to inhibit differentiation, HPV16 oncoproteins, E6 and E7, were reported to play a central role.<sup>5,6</sup> It has been proposed that MAML1, NOTCH, and PTPN14 are key molecules that mediate the inhibitory effects of high-risk HPV oncoproteins on squamous differentiation.<sup>3,7,8,28,31</sup> However, the precise mechanisms controlled by both oncoproteins remain unknown. We detected the significant promotion of *NOTCH3* expression in FOXP4-suppressed W12 cells by microarray and WAD ranking methods.<sup>23</sup> Although it has been reported that *NOTCH3* expression is induced by *ELF3* transcription factor<sup>32</sup> and promotes the expression of the *HES* family,<sup>33</sup> there has been no report describing the possible relationship between HPV-impaired squamous differentiation and FOXP4.<sup>3</sup> This study first showed that *ELF3* is involved in FOXP4-dependent pathways to suppress squamous differentiation and suggests suppressive roles for *ELF3* and *NOTCH3* in CIN progression.

As normal uterine cervical squamous cell lines were not available, we used an immortalized human keratinocyte cell line, HaCaT cells,

which have been reported to undergo squamous differentiation in the presence of a high extracellular calcium concentration.<sup>34,35</sup> Using HaCaT cells transfected with E5, E6, or E7, Bergner et al. found that the E7 oncogene, with the contribution of E6, but not E5, influenced cell morphology and differentiation in HaCaT cells.<sup>36</sup> In this study, we demonstrated that FOXP4 regulates squamous differentiation through *ELF3* and *NOTCH3* in HaCaT cells. This result suggests the involvement of the FOXP4-*ELF3* pathway in physiological squamous differentiation. The present study showed that FOXP4 is transiently expressed in normal squamous-lineage cells, such as reserve cells and immature stratified squamous cells, during squamous metaplasia. Considering that reserve cells have been proposed to be stem cells of CIN and uterine cervical cancer,<sup>37,38</sup> we suggest that FOXP4 is a unique target molecule that can regulate the cellular behavior of HPV-infected stem cells.

Recently, a long noncoding RNA (lncRNA), FOXP4-antisense RNA 1 (FOXP4-AS1), was reported to be involved in cancer prognosis.<sup>39</sup> Using uterine cervical cancer cell lines, FOXP4-AS1 was demonstrated to be involved in cell proliferation, migration, and invasion.<sup>40</sup> In addition, FOXP4-AS1 was shown to positively regulate FOXP4 by stabilizing FOXP4 mRNA and upregulating the expression of FOXP4 by sponging miR-3184-5p, and to promote the proliferation of esophageal SCC.<sup>41</sup> The cooperation of other lncRNA SNHG16 and miR-877-5p in the induction of FOXP4 expression on

**FIGURE 9** Estimated roles of FOXP4 in the proliferation and squamous differentiation in the uterine cervix. FOXP4 promotes proliferation and inhibits squamous differentiation through ELF3 and NOTCH3 in human uterine cervical epithelial cells, which may regulate squamous metaplasia and CIN progression. This indicates that FOXP4 is a candidate target molecule for differentiation therapy of CIN



laryngeal SCC was also reported.<sup>42</sup> Conversely, the somatic mutation of *ELF3* was reported in uterine cervical adenocarcinomas<sup>43</sup> and urothelial bladder carcinoma,<sup>44</sup> and significant loss of *ELF3* immunostaining was observed in oral SCC.<sup>45</sup> *ELF3* was also reported to be one of the driver genes for ampullary carcinomas.<sup>46</sup> Although the pathological relationship of *FOXP4* and *ELF3* in uterine cervical SCC is still unknown, this study showed the sequential expression of *FOXP4* and *ELF3* (from *FOXP4* to *ELF3*) during the differentiation process in normal, CIN1, and CIN2 lesions using immunohistochemical staining (Figures 1B-a-d and 6C-a-c). However, this sequential expression pattern was lost in CIN3 (Figures 1B-e and 6C-d), suggesting that the differentiation-regulating pathway by *FOXP4*-*ELF3* had already been disrupted in CIN3.

A limitation of our study was the lack of animal experiments. As animal cells are not natural hosts for HPV, the use of an animal model of CIN under HPV infection is difficult. Consequently, we used a raft culture system that was reported to exhibit dysplastic lesions using human keratinocytes infected with HPV, which is also similar to those observed in *in vivo* CIN regions.<sup>24,25</sup>

In conclusion, this study suggests the physiological role of *FOXP4* in squamous metaplasia and the pathological role in CIN progression (Figure 9). Using *in vitro* culture experiments, this study indicated that the suppression of *FOXP4* gene expression attenuated the proliferation of CIN-derived W12 cells. This treatment also promoted their squamous differentiation through an *ELF3*-dependent pathway. From these findings, we propose that *FOXP4* is a novel target molecule for the nonsurgical differentiation therapy of CIN, which suppresses the growth of HPV-infected lesions by inducing further differentiation toward the mature phenotype. This strategy from a novel viewpoint may also contribute to developing a new therapy for other HPV-related diseases including benign tumors.

#### AUTHOR CONTRIBUTIONS

MN, JT, TD, and HF conceived the study and study design; KN, JI, MO, and YM prepared clinical samples; TM, TI, TO, AM, and KK performed the experiments and data analysis; TM and HF wrote the paper; TM, MN, KY, MM, SK, CT, and HF discussed and revised the paper; HF was the originator of the concept of this report and approved the paper. All of the authors approved this paper.

#### ACKNOWLEDGMENTS

The authors are grateful to Ms. Ai Sato and Ms. Mai Kawakita for their technical assistance and preparation of the manuscript. We also thank Drs Paul Lambert, Tomomi Nakahara, and Iwao Kukimoto for the W12 cell line.

#### FUNDING INFORMATION

This work was supported in part by Grants-in-Aid for Scientific Research (nos. 17H04337, 19H01617, 19K22681, 20H03822, and 21H04837) and the Japan Agency for Medical Research and Development (no. 20ck0106549h0001).

#### DISCLOSURE

The authors declare no competing interests.

#### DATA AVAILABILITY STATEMENT

All data generated or analyzed during this study are included in this published article. The data that support the findings of this study are available from the corresponding author upon reasonable request.

#### ETHICAL APPROVAL AND CONSENT TO PARTICIPATE

All protocols were approved by the Medical Ethics Committee of Kanazawa University (approval number: 2015-085). Human studies were conducted according to the Declaration of Helsinki principles, and written informed consent was received from participants prior to inclusion in the study.

#### ORCID

Takashi Iizuka <https://orcid.org/0000-0003-1885-6272>

Satoru Kyo <https://orcid.org/0000-0002-8986-6147>

Yasunari Mizumoto <https://orcid.org/0000-0001-8648-3696>

Hiroshi Fujiwara <https://orcid.org/0000-0003-3098-9406>

#### REFERENCES

- Walboomers JM, Jacobs MV, Manos MM, et al. Human papillomavirus is a necessary cause of invasive cervical cancer worldwide. *J Pathol.* 1999;189:12-19.
- Graham SV. Keratinocyte differentiation-dependent human papillomavirus gene regulation. *Viruses.* 2017;9:245.

3. White EA. Manipulation of epithelial differentiation by HPV oncoproteins. *Viruses*. 2019;11:369.
4. Buckley CH, Butler EB, Fox H. Cervical intraepithelial neoplasia. *J Clin Pathol*. 1982;35:1-13.
5. Zehbe I, Richard C, DeCarlo CA, et al. Human papillomavirus 16 E6 variants differ in their dysregulation of human keratinocyte differentiation and apoptosis. *Virology*. 2009;383:69-77.
6. Nees M, Geoghegan JM, Munson P, et al. Human papillomavirus type 16 E6 and E7 proteins inhibit differentiation-dependent expression of transforming growth factor-beta2 in cervical keratinocytes. *Cancer Res*. 2000;60:4289-4298.
7. Hatterschide J, Bohidar AE, Grace M, et al. PTPN14 degradation by high-risk human papillomavirus E7 limits keratinocyte differentiation and contributes to HPV-mediated oncogenesis. *Proc Natl Acad Sci USA*. 2019;116:7033-7042.
8. Meyers JM, Uberoi A, Grace M, Lambert PF, Munger K. Cutaneous HPV8 and MmuPV1 E6 proteins target the NOTCH and TGF-beta tumor suppressors to inhibit differentiation and sustain keratinocyte proliferation. *PLoS Pathog*. 2017;13:e1006171.
9. Iizuka T, Wakae K, Nakamura M, et al. APOBEC3G is increasingly expressed on the human uterine cervical intraepithelial neoplasia along with disease progression. *Am J Reprod Immunol*. 2017;78:e12703.
10. Wakae K, Aoyama S, Wang Z, et al. Detection of hypermutated human papillomavirus type 16 genome by next-generation sequencing. *Virology*. 2015;485:460-466.
11. Yang T, Li H, Thakur A, et al. FOXP4 modulates tumor growth and independently associates with miR-138 in non-small cell lung cancer cells. *Tumour Biol*. 2015;36:8185-8191.
12. Takata R, Akamatsu S, Kubo M, et al. Genome-wide association study identifies five new susceptibility loci for prostate cancer in the Japanese population. *Nat Genet*. 2010;42:751-754.
13. Liu M, Shi X, Wang J, et al. Association of FOXP4 gene with prostate cancer and the cumulative effects of rs4714476 and 8q24 in Chinese men. *Clin Lab*. 2015;61:1491-1499.
14. Wang G, Sun Y, He Y, Ji C, Hu B, Sun Y. MicroRNA-338-3p inhibits cell proliferation in hepatocellular carcinoma by target forkhead box P4 (FOXP4). *Int J Clin Exp Pathol*. 2015;8:337-344.
15. Golson ML, Kaestner KH. Fox transcription factors: from development to disease. *Development*. 2016;143:4558-4570.
16. Hannehalli S, Kaestner KH. The evolution of Fox genes and their role in development and disease. *Nat Rev Genet*. 2009;10:233-240.
17. Li S, Wang Y, Zhang Y, et al. Foxp1/4 control epithelial cell fate during lung development and regeneration through regulation of anterior gradient 2. *Development*. 2012;139:2500-2509.
18. Wakae K, Nishiyama T, Kondo S, et al. Keratinocyte differentiation induces APOBEC3A, 3B, and mitochondrial DNA hypermutation. *Sci Rep*. 2018;8:9745.
19. Boukamp P, Petrussevska RT, Breitkreutz D, Hornung J, Markham A, Fusenig NE. Normal keratinization in a spontaneously immortalized aneuploid human keratinocyte cell line. *J Cell Biol*. 1988;106:761-771.
20. Choo CK, Rorke EA, Eckert RL. Differentiation-independent constitutive expression of the human papillomavirus type 16 E6 and E7 oncogenes in the CaSki cervical tumour cell line. *J Gen Virol*. 1994;75(Pt 5):1139-1147.
21. Breitkreutz D, Stark HJ, Plein P, Baur M, Fusenig NE. Differential modulation of epidermal keratinization in immortalized (HaCaT) and tumorigenic human skin keratinocytes (HaCaT-ras) by retinoic acid and extracellular Ca<sup>2+</sup>. *Differentiation*. 1993;54:201-217.
22. Stanley MA, Browne HM, Appleby M, Minson AC. Properties of a non-tumorigenic human cervical keratinocyte cell line. *Int J Cancer*. 1989;43:672-676.
23. Kadota K, Nakai Y, Shimizu K. A weighted average difference method for detecting differentially expressed genes from microarray data. *Algorithms Mol Biol*. 2008;3:8.
24. Anacker D, Moody C. Generation of organotypic raft cultures from primary human keratinocytes. *J Vis Exp*. 2012;3668. doi:10.3791/3668
25. Wilson R, Laimins LA. Differentiation of HPV-containing cells using organotypic "raft" culture or methylcellulose. *Methods Mol Med*. 2005;119:157-169.
26. Doorbar J, Griffin H. Refining our understanding of cervical neoplasia and its cellular origins. *Papillomavirus Res*. 2019;7:176-179.
27. Scheffner M, Munger K, Byrne JC, Howley PM. The state of the p53 and retinoblastoma genes in human cervical carcinoma cell lines. *Proc Natl Acad Sci USA*. 1991;88:5523-5527.
28. Yugawa T, Handa K, Narisawa-Saito M, Ohno S, Fujita M, Kiyono T. Regulation of Notch1 gene expression by p53 in epithelial cells. *Mol Cell Biol*. 2007;27:3732-3742.
29. Herfs M, Yamamoto Y, Laury A, et al. A discrete population of squamocolumnar junction cells implicated in the pathogenesis of cervical cancer. *Proc Natl Acad Sci USA*. 2012;109:10516-10521.
30. Herfs M, Vargas SO, Yamamoto Y, et al. A novel blueprint for 'top down' differentiation defines the cervical squamocolumnar junction during development, reproductive life, and neoplasia. *J Pathol*. 2013;229:460-468.
31. Lefort K, Mandinova A, Ostano P, et al. Notch1 is a p53 target gene involved in human keratinocyte tumor suppression through negative regulation of ROCK1/2 and MRCKalpha kinases. *Genes Dev*. 2007;21:562-577.
32. Ali SA, Justilien V, Jamieson L, Murray NR, Fields AP. Protein kinase Ciota drives a NOTCH3-dependent stem-like phenotype in mutant KRAS lung adenocarcinoma. *Cancer Cell*. 2016;29:367-378.
33. Xiao G, Du J, Wu H, et al. Differential inhibition of Sox10 functions by Notch-Hes pathway. *Cell Mol Neurobiol*. 2020;40:653-662.
34. Yuspa SH, Hennings H, Tucker RW, Jaken S, Kilkenny AE, Roop DR. Signal transduction for proliferation and differentiation in keratinocytes. *Ann N Y Acad Sci*. 1988;548:191-196.
35. Deyrieux AF, Wilson VG. In vitro culture conditions to study keratinocyte differentiation using the HaCaT cell line. *Cytotechnology*. 2007;54:77-83.
36. Bergner S, Halec G, Schmitt M, Aubin F, Alonso A, Auvinen E. Individual and complementary effects of human papillomavirus oncogenes on epithelial cell proliferation and differentiation. *Cells Tissues Organs*. 2016;201:97-108.
37. Smedts F, Ramaekers FC, Hopman AH. The two faces of cervical adenocarcinoma in situ. *Int J Gynecol Pathol*. 2010;29:378-385.
38. Sato M, Kawana K, Adachi K, et al. Regeneration of cervical reserve cell-like cells from human induced pluripotent stem cells (iPSCs): a new approach to finding targets for cervical cancer stem cell treatment. *Oncotarget*. 2017;8:40935-40945.
39. Huang Y, Ling A, Pareek S, Huang RS. Oncogene or tumor suppressor? Long noncoding RNAs role in patient's prognosis varies depending on disease type. *Transl Res*. 2020;230:98-110.
40. Zhao J, Yang T, Li L. LncRNA FOXP4-AS1 is involved in cervical cancer progression via regulating miR-136-5p/CBX4 Axis. *Onco Targets Ther*. 2020;13:2347-2355.
41. Li Y, Li T, Yang Y, Kang W, Dong S, Cheng S. YY1-induced upregulation of FOXP4-AS1 and FOXP4 promote the proliferation of esophageal squamous cell carcinoma cells. *Cell Biol Int*. 2020;44:1447-1457.
42. Wang X, Liu L, Zhao W, Li Q, Wang G, Li H. LncRNA SNHG16 promotes the progression of laryngeal squamous cell carcinoma by mediating miR-877-5p/FOXP4 Axis. *Onco Targets Ther*. 2020;13:4569-4579.

43. Ojesina AI, Lichtenstein L, Freeman SS, et al. Landscape of genomic alterations in cervical carcinomas. *Nature*. 2014;506:371-375.
44. Cancer Genome Atlas Research Network. Comprehensive molecular characterization of urothelial bladder carcinoma. *Nature*. 2014;507:315-322.
45. AbdulMajeed AA, Dalley AJ, Farah CS. Loss of ELF3 immunoeexpression is useful for detecting oral squamous cell carcinoma but not for distinguishing between grades of epithelial dysplasia. *Ann Diagn Pathol*. 2013;17:331-340.
46. Yachida S, Wood LD, Suzuki M, et al. Genomic sequencing identifies ELF3 as a driver of ampullary carcinoma. *Cancer Cell*. 2016;29:229-240.

**How to cite this article:** Matsumoto T, Iizuka T, Nakamura M, et al. FOXP4 inhibits squamous differentiation of atypical cells in cervical intraepithelial neoplasia via an ELF3-dependent pathway. *Cancer Sci*. 2022;113:3376-3389. doi: [10.1111/cas.15489](https://doi.org/10.1111/cas.15489)